



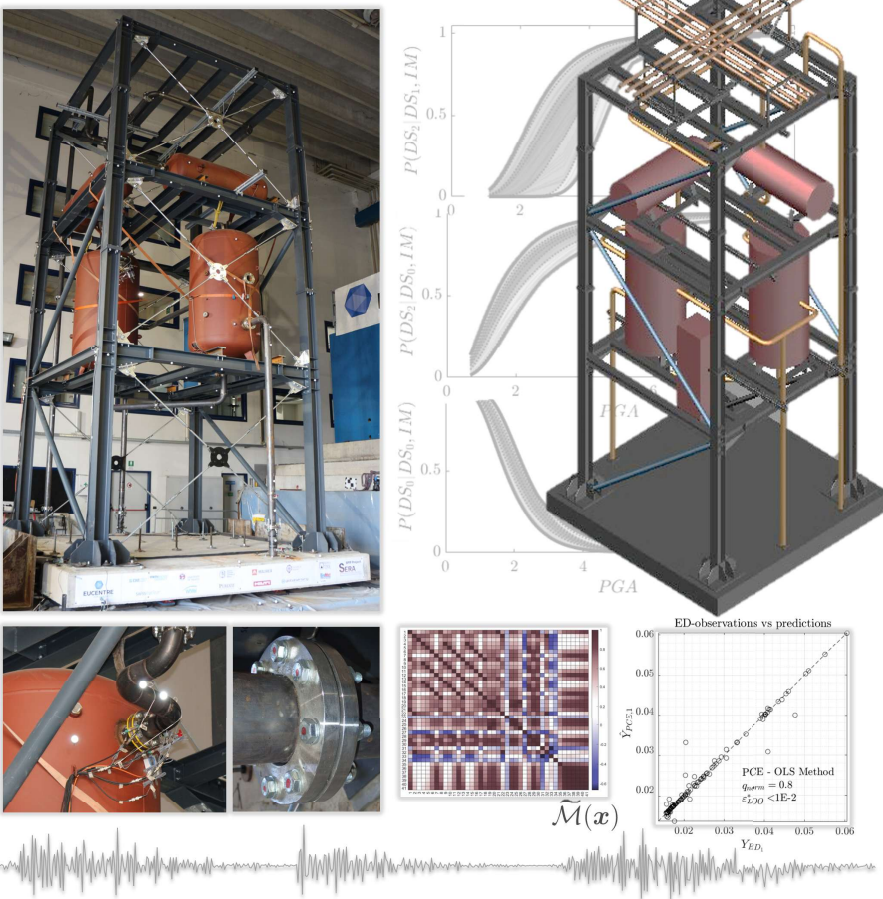
UNIVERSITY OF TRENTO

Doctoral School in Civil, Environmental and  
Mechanical Engineering

Curriculum 3. Modelling and Simulation

Chiara Nardin

# Seismic experimental analyses and surrogate models of multi-component systems in special-risk industrial facilities







UNIVERSITY  
OF TRENTO

**Doctoral School in Civil, Environmental  
and Mechanical Engineering**

**Curriculum *Modelling and Simulation*  
XXXV cycle - 2019-2022**

**Doctoral Thesis - December 2022**

**Seismic experimental analyses and surrogate models  
of multi-component systems in special-risk industrial facilities**

**Supervisor**

Prof. Oreste S. Bursi

**Ph.D. Candidate**

Chiara Nardin

Credits of the cover image belong to the SPIF Project and the University of Trento.



Except where otherwise noted, contents on this book are licensed under a Creative  
Common Attribution - Non Commercial - No Derivatives  
4.0 International License

University of Trento  
Doctoral School in Civil, Environmental and Mechanical Engineering  
<http://web.unitn.it/en/dricam>  
Via Mesiano 77, I-38123 Trento  
Tel. +39 0461 282670 / 2611 - [dicamphd@unitn.it](mailto:dicamphd@unitn.it)

*If you want to find the secrets of the universe, think in terms of energy,  
frequency and vibration.*

*Se vuoi scoprire i segreti dell'universo, pensa in termini di energia,  
frequenza e vibrazione.*

Nikola Tesla



## Acknowledgements

I want to seize this moment to thank all who shared with me and made it possible to complete this PhD journey: if I leave out some names here, I certainly will not forget my memories of our experiences together.

First of all, I would like to thank my Supervisor and Professor Oreste S. Bursi, for his guidance in this up-to-date learning experience and for sharing invaluable work and life-related lessons with me.

A special thanks to Marco Broccardo for his advice, talks and sharing of experiences and ideas on research. Thank you for letting me discover the amazing world of ETH and the RSUQ group led by Professor Bruno Sudret and Stefano Marelli. I got to know a dynamic environment full of continuous interactions, built up of unique and incredible people, among whom undoubtedly Stefano, Nora, Katerina, Anderson and the whole group.

I would also like to thank UNITN: from fellow students first, to colleagues and dear friends later, a special mention goes to Giulia, Roberto, Luca, Patrick and many others without whom I would not have achieved so many goals.

A due thank you to my new and lifelong friends, Maria, Alison, Andrea, Daniele, Margherita, Arianna and all, who have supported and sustained me on this journey...even with massive 5kg each for 600km! I am lucky to have you as my friends.

Last but not least, a grateful thank you to my family: without you, none of this would have been possible. Thank you for being there at all times, thank you for the values with which you have raised me and for the continuous care and unconditional love that you donate. A special memory goes out to my grandparents, Alba and Luigi, AnnaMaria and Renzo, to whom I dedicate this thesis: thank you for always being with me.

*Chiara*



## **Ringraziamenti**

Vorrei cogliere questo momento per ringraziare tutti coloro che mi hanno permesso di portare a termine e hanno condiviso con me questo percorso di Dottorato: se qualche nome qui tralascio, di sicuro lo porto con me nei ricordi delle esperienze vissute insieme.

Innanzitutto desidero ringraziare il mio relatore e Professore Oreste S. Bursi, per avermi guidato in questa esperienza formativa e aver condiviso con me preziosi insegnamenti, sia lavorativi che di vita. Un grazie speciale a Marco Broccardo, per i suoi consigli, le chiacchierate ed aver condiviso scambi ed idee sulla ricerca. Grazie, per avermi consentito di conoscere il meraviglioso mondo di ETH e del gruppo RSUQ guidato dal Professor Bruno Sudret e Stefano Marelli. Ho avuto modo di conoscere una realtà dinamica e ricca di continui scambi, fatta di persone speciali ed incredibili, fra cui indubbiamente Stefano, Nora, Katerina, Anderson e tutto il gruppo.

Non da meno, desidero ringraziare anche la realtà Unitn: da compagni di studio prima, a colleghi e cari amici poi, una menzione speciale la trovano Giulia, Roberto, Luca, Patrick e tutti coloro senza i quali non avrei raggiunto tanti obiettivi.

Un ringraziamento doveroso agli amici nuovi e di sempre, Maria, Alison, Andrea, Daniele, Margherita, Arianna e tutti, che mi hanno sostenuto e supportato in questo viaggio..portando addirittura ben 5kg a testa per 600km! Sono fortunata ad avervi come amici.

Infine, non da ultimo, un doveroso grazie alla mia famiglia: senza di voi, nulla di tutto questo sarebbe stato mai possibile. Grazie per esserci in qualsiasi momento, grazie per i valori con cui mi avete cresciuta e per il continuo affetto e amore incondizionato che donate. Un pensiero speciale lo rivolgo ai miei nonni, Alba e Luigi, AnnaMaria e Renzo a cui dedico questo lavoro: grazie per essere sempre con me.

*Chiara*



## Abstract

Nowadays, earthquakes are one of the most catastrophic natural events that have a significant human, socio-economic and environmental impact. Besides, based on both observations of damage following recent major/moderate seismic events and numerical/experimental studies, it clearly emerges that critical non-structural components (NSCs) that are ubiquitous to most industrial facilities are particularly and even disproportionately vulnerable to those events. Nonetheless and despite their great importance, seismic provisions for industrial facilities and their process equipment are still based on the classical load-and-resistance factor design (LRFD) approach; a performance-based earthquake engineering (PBEE) approach should, instead, be preferred. Along this vein, in recent years, much research has been devoted to setting computational fragility frameworks for special-risk industrial components and structures. However, within a PBEE perspective, studies have clearly remarked: i) a lack of definition of performance objectives for NSCs; ii) the need for fully comprehensive testing campaigns data on coupling effects between main structures and NSCs.

In this respect, this doctorate thesis introduces a computational framework for an efficient and accurate seismic state-dependent fragility analysis; it is based on a combination of data acquired from an extensive experimental shake table test campaign on a full-scale prototype industrial steel frame structure and the most recent surrogate-based UQ forward analysis advancements.

Specifically, the framework is applied to a real-world application consisting of seismic shake table tests of a representative industrial multi-storey frame structure equipped with complex process components, carried out at the EUCENTRE facility in Italy, within the European SPIF project: Seismic Performance of Multi-Component Systems in Special Risk Industrial Facilities.

The results of this experimental research campaign also aspire to improve the understanding of these complex systems and improve the knowledge of FE modelling techniques. The main goals aim to reduce the huge computational burden and to assess, as well, when the importance of coupling effects between NSCs and the main structure comes into play. Insights provided by innovative monitoring systems were then deployed to develop and validate numerical and analytical models.

At the same time, the adoption of Der Kiureghian's stochastic site-based ground motion model (GMM) was deemed necessary to severely excite the process equipment and supplement the scarcity of real records

---

with a specific frequency content capable of enhancing coupling effects.

Finally, to assess the seismic risk of NSCs of those special facilities, this thesis introduces state-dependent fragility curves that consider the accumulation of damage effects due to sequential seismic events. To this end, the computational burden was alleviated by adopting polynomial chaos expansion (PCE) surrogate models. More precisely, the dimensionality of a seismic input random vector has been reduced by performing the principal component analysis (PCA) on the experimental realizations. Successively, by bootstrapping on the experimental design, separate PCE coefficients have been determined, yielding a full response sample at each point. Eventually, empirical state-dependent fragility curves were derived.

## Publications

As a result of the work conducted in this thesis, the following publications have been produced:

### Journal Publications:

- J-1** Paolacci, F., Quinci, G., **C. Nardin**, Vezzari, V., Marino, A., Ciucci, M., (2021). Bolted Flange Joints equipped with FBG sensors in industrial piping Systems subject to seismic loads. *Journal of Loss Prevention in the Process Industries*. doi.org/10.1016/j.jlp.2021.104576
- J-2** C. Butenweg, O.S. Bursi, F. Paolacci, I. Lanese, M. Marinkovic, **C. Nardin**, G. Quinci (2021). Seismic performance of an industrial multi-storey frame structure with process equipment subjected to shake table testing. *Engineering Structure*. doi.org/10.1016/j.engstruct.2021.112681
- J-3** **C. Nardin**, O.S. Bursi, F. Paolacci, A. Pavese, G. Quinci (2022). Experimental performance of a multi-storey braced frame structure with non-structural industrial components subjected to synthetic ground motions. *Earthquake Engineering & Structural Dynamics*. doi.org/10.1002/eqe.3656
- J-4** G. Quinci, **C. Nardin**, F. Paolacci, O.S. Bursi (2022). Modelling issues in seismic risk analysis of Non-Structural Components installed on industrial plant subsystems. *Bullettin of Earthquake Engineering. (under submission)*
- J-5** **C. Nardin**, S. Marelli, O.S. Bursi (2023). Meta-model state-dependent demand fragility curves for non-structural components in special risk industrial facilities. *Earthquake Engineering & Structural Dynamics. (in progress)*

### Conferences:

- C-1** **C. Nardin**, R. di Filippo, R. Endrizzi, I. Lanese, F. Paolacci, O.S. Bursi (2020). Ground Motion Model For Seismic Vulnerability Assessment Of Portotype Industrial Plants. *Proceedings of the ASME 2020 Pressure Vessels & Piping Conference PVP2020*, July 19-24 2020 Minneapolis, Minnesota, USA.

---

**C-2** C. Butenweg, O.S. Bursi, **C. Nardin**, I. Lanese, A. Pavese, M. Marinkovic, F. Paolacci, G. Quinci (2020). Simulated Investigation On The Seismic Performance Of A Multi-Component System For Major-Hazard Industrial Facilities. *Proceedings of the ASME 2020 Pressure Vessels & Piping Conference PVP2020*, July 19-24 2020 Minneapolis, Minnesota, USA.

**C-3** C. Butenweg, M. Marinkovic, A. Pavese, I. Lanese, B. Hoffmeister, M. Pinkawa, C. Vulcu, O. S. Bursi, **C. Nardin**, F. Paolacci, G. Quinci, M. Fragiadakis, F. Weber, P. Huber, P. Renault, M. Gündel, S. Dyke, M. Ciucci, A. Marino (2020). Simulated Investigation On The Seismic Performance Of A Multi-Component System For Major-Hazard Industrial Facilities. *17th World Conference on Earthquake Engineering, 17WCEE*, September 13-18 2020 Sendai, Japan.

**C-4** **C. Nardin**, R. di Filippo, R. Endrizzi, I. Lanese, F. Paolacci, O.S. Bursi (2020). A Ground Motion Model For Seismic Vulnerability Assessment Of Portotype Industrial Plants. *EURODYN 2020 - XI International Conference on Structural Dynamics*, 23—25 November 2020 Athens, Greece.

**C-5** C. Butenweg, O.S. Bursi, I. Lanese, M. Marinkovic, **C. Nardin**, F. Paolacci, A. Pavese, G. Quinci (2021). Experimental Investigation on the Seismic Performance of a Multi-Component System for Major-Hazard Industrial Facilities. *Proceedings of the Online ASME 2021 Pressure Vessels & Piping Conference PVP2021*, June 12-16 2021, Virtual Conference.

**C-6** **C. Nardin**, O.S. Bursi, I. Lanese, A. Pavese, F. Paolacci, G. Quinci (2021). Shake Table Testing for a Multi-Component Prototype Industrial Plant: Input and System Modelling Issues. *Proceedings of the Online ASME 2021 Pressure Vessels & Piping Conference PVP2021*, June 12-16 2021, Virtual Conference.

## Projects:

**P-1** *Seismic Performance of Multi-Component Systems in Special Risk Industrial Facilities (SPIF)*, European Union's Horizon 2020 Research and Innovation Programme - Grant Agreement No. 730900.

**Deliverables:**

- D-1** D10.1 - Technical report on SERA Transnational Access activities TA1-TA10 M36, Project #34 – *Seismic Performance of multi-component systems in special risk Industrial Facilities* (SPIF).



## Contents

<b>1</b>	<b>Introduction</b>	<b>3</b>
1.1	Background and motivation . . . . .	3
1.2	Objectives of the thesis and core contribution . . . . .	8
1.3	Organization of the thesis . . . . .	9
<b>2</b>	<b>Experimental performance of multi-storey MR frame structure with process equipment subjected to artificial ground motions</b>	<b>15</b>
2.1	Introduction . . . . .	16
2.1.1	Background and Motivation . . . . .	16
2.1.2	Scope . . . . .	20
2.2	Experimental Mock-up and Setup . . . . .	20
2.2.1	Mock-up Description . . . . .	20
2.2.2	Sensors Layout . . . . .	26
2.3	Selection of seismic input and Test Programme . . . . .	29
2.3.1	Performance Based Design and Reference Limit States . . . . .	29
2.3.2	Spectrum-compatible Accelerograms . . . . .	30
2.3.3	Test Programme . . . . .	31
2.4	System Identification and Observations . . . . .	34
2.4.1	Identification of frequencies, mode shapes and damping ratios . . . . .	34
2.4.2	System performance . . . . .	39
	Main structure response and damage . . . . .	39
	NSC system response and damage . . . . .	40
2.5	Data Analysis and Insights . . . . .	50
2.5.1	Floor response and literature comparisons . . . . .	50
2.5.2	Structural regularity considerations . . . . .	54
2.6	Conclusions and future developments . . . . .	57
<b>3</b>	<b>Experimental performance of multi-storey BF frame structure with process equipment subjected to site-based ground motions</b>	<b>63</b>
3.1	Introduction . . . . .	64
3.1.1	Background and Motivation . . . . .	64
3.1.2	Scope . . . . .	67
3.2	The Project SPIF: Learned Lessons from a multi-storey Moment Resisting Frame . . . . .	69

---

3.2.1	The Case Study . . . . .	69
3.2.2	Seismic Inputs . . . . .	70
3.2.3	Main Results . . . . .	70
3.3	The Project SPIF #2: Performance of a multi-storey braced frame . . . . .	73
3.3.1	Rationale . . . . .	73
3.3.2	Performance based design and reference limit states	75
3.3.3	FE model of the primary steel structure . . . . .	78
3.3.4	FE models of the piping systems and secondary elements . . . . .	79
3.4	Input Selection, Shake Table Test Programme and Sensor Layout . . . . .	82
3.4.1	Input Selection . . . . .	82
3.4.2	Test programme . . . . .	85
3.4.3	Sensor layout . . . . .	85
3.5	Data Analysis and Insight . . . . .	88
3.5.1	System ID of frequencies, mode shapes and damping ratios of the primary structure . . . . .	88
3.5.2	Performance of the Primary Structure . . . . .	90
3.5.3	Behaviour of Secondary Components . . . . .	92
3.5.4	Correlations between input, primary structure and non-structural components . . . . .	97
3.6	Conclusions and outlooks . . . . .	102
<b>4</b>	<b>Fiber Bragg Grating sensors performance in Bolted Flange Joints of piping systems under seismic conditions</b>	<b>107</b>
4.1	Introduction . . . . .	108
4.1.1	Background and Motivation . . . . .	108
4.1.2	Scope . . . . .	110
4.2	Related work . . . . .	111
4.3	Use of optical fibers for seismic monitoring of Bolted Flange Joints . . . . .	112
4.4	Experimental investigation on an isolated Bolted Flange Joint . . . . .	117
4.4.1	Description of Case study #1 . . . . .	117
4.4.2	Description of the mock-up and the sensors layout	118
4.4.3	Description of the test setup . . . . .	120
4.4.4	Results . . . . .	124
4.5	Experimental investigation on Bolted Flange Joints part of an industrial plant substructure . . . . .	130
4.5.1	Description of Case study #2 . . . . .	130
4.6	Summary and conclusions . . . . .	135

<b>5 High fidelity model and seismic risk analysis of a vertical tank</b>	<b>141</b>
5.1 Introduction . . . . .	142
5.1.1 Background and Motivation . . . . .	142
5.1.2 Scope . . . . .	144
5.2 Description of the cases study . . . . .	145
5.3 Multi-Storey frame and equipment modelling issues . . . . .	148
5.3.1 Main Steel Frame Structure . . . . .	148
5.3.2 Piping systems and non structural components . . . . .	150
5.4 Numerical Simulations and Comparison with Experimental Results . . . . .	155
5.4.1 Free vibration analyses and model calibration . . . . .	155
5.4.2 Seismic response analysis and results comparison	158
5.5 Seismic vulnerability analysis of industrial multi-storey frame structures . . . . .	162
5.5.1 Input selection . . . . .	162
5.5.2 Fragility assessment . . . . .	165
5.5.3 Risk assessment and discussion of the results . . . . .	169
5.6 Summary and Conclusions . . . . .	171
<b>6 Metamodel state-dependent demand fragility curves for process equipment in industrial facilities</b>	<b>179</b>
6.1 Introduction . . . . .	180
6.1.1 Background and motivation . . . . .	180
6.1.2 Scope and core contribution . . . . .	182
6.2 Seismic fragility analyses framework . . . . .	183
6.2.1 Theoretical background . . . . .	183
6.2.2 Step $\mathcal{B}$ - Input Parameters . . . . .	185
6.2.3 Step $\mathcal{A}_2$ - PCE metamodel . . . . .	189
6.2.4 Step $\mathcal{C}$ - Fragility analysis . . . . .	190
6.3 The case studies . . . . .	190
6.3.1 The MDof shear-type system with Bouc-Wen hysteresis . . . . .	191
6.3.2 The steel BF structure endowed with industrial process NSCs . . . . .	191
6.4 Computational numerical and FE models . . . . .	192
6.4.1 Numerical MDof shear-type system model . . . . .	192
6.4.2 FE physics-informed model for SPIF #2 . . . . .	193
6.5 Seismic fragility analyses . . . . .	196
6.5.1 Benchmark: the MDof system with Bouc-Wen model . . . . .	196
Monte Carlo Analyses: Fragility Functions . . . . .	196
PCE metamodel: fragility functions . . . . .	198

---

Validation of the method's outcomes . . . . .	202
6.5.2    Industrial NSC state-dependent fragility functions:	
the SPIF #2 vertical tank . . . . .	203
Bootstrapped-PCE metamodel . . . . .	203
Comparison between the Lognormal and the Em-	
pirical distribution . . . . .	206
6.6    Conclusions and future developments . . . . .	208
A.    Histograms and distributional models: input meta-features.	210
B.    Inferred distribution of the state-dependent fragility func-	
tions for the NSC. . . . .	216
<b>7    Summary, conclusions and future perspectives</b>	<b>223</b>
7.1    Summary and discussion of research results . . . . .	223
7.2    Future perspectives . . . . .	225
<b>A    Some considerations on Markovian Processes.</b>	<b>227</b>
A.1    Introduction . . . . .	227
A.2    Theoretical Background . . . . .	227
A.3    State-dependent fragility functions . . . . .	230

## List of Figures

1.1	PBEE schematics: minimum seismic performance objectives coupled with earthquake levels for buildings, according to [7]. . . . .	4
1.2	The PEER-PBEE schematics. . . . .	6
2.1	Mock-up photographs at the EUCENTRE Laboratory. . . . .	19
2.3	Primary steel structure . . . . .	22
2.4	Typical anchorage of columns to the reinforced concrete plate: base plate with welded stiffeners and anchors. . . . .	23
2.5	Geometry of the vertical (a) and horizontal (b) tanks . . . . .	24
2.7	Piping system and layout . . . . .	25
2.8	Pipe rack on the third floor . . . . .	26
2.9	Sensors location at each floor . . . . .	27
2.10	Piping monitoring: sensors location on the BFJs . . . . .	28
2.11	Markers layout . . . . .	29
2.12	Eurocode 8-Part 1 Target spectrum and artificially generated spectrum for time histories TH #8. . . . .	30
2.14	Acquired signal and PSDs either on MRF and BF direction for Random #13 - excitation at the beginning of the test programme - and Random #18 - excitation at the end of the test campaign -, respectively: a shift to the left of frequencies especially those in the BF direction is evident.	36
2.15	a) Relevant frequency variations for the mock-up. Damping ratio box-plots are reported with whiskers referring to the 10 <sup>th</sup> and 90 <sup>th</sup> -quantile; b) mode shapes relevant to frequencies $f_n = 2.88 - 4.24 - 6.38 - 9.17 \text{ Hz}$ of Table 2.7. . . . .	42
2.16	Frequency response functions and coherence $C_{xy}(\omega)$ for the record TH #8-25% both for the MRF direction and the BF direction. . . . .	43
2.18	Strain values of base columns vs. PGA recorded by strain gauges for different seismic records . . . . .	45
2.19	Additional bolted tee stub used to connect the crossbeam to the main beam. . . . .	45

---

2.20	Cracks and warping of fin plate connections between primary MRF beam and secondary crossbeams at the first floor: (a) Cracking and warping of fin plate FP #1 during TH #8-70% ; (b) Damage of fin plate FP #2 during TH #8-100%; (c) Cracks and warping of fin plate FP #2 during TH #8-110%. . . . .	46
2.21	Collapse of the supporting system of the conveyor at base level for record TH #8-110% . . . . .	46
2.22	Collapse of the pipe rack at the third floor. . . . .	47
2.23	Floors motion recorded by means of marker sensors for the record TH #8-110% . . . . .	47
2.24	Comparison of time histories for Tank #2 and Tank #4 subjected to the record TH #8-110%: a) acceleration; b) relative displacement . . . . .	48
2.25	(a) Acceleration time history of the sensor A #13 of the cabinet at Level 1 for the record TH #8-110% and (b) relevant frequency spectrum . . . . .	49
2.26	Experimental floor response spectra for TH #8-50% and TH #8-110% seismic excitations . . . . .	51
2.27	Comparison between analytical and experimental floor response spectra for the Record TH #8-110% . . . . .	52
2.28	Acceleration and displacement profiles for different THs . . . . .	53
2.29	Acceleration profiles of Tank #2 and Tank #3 for different PGA levels of TH #8. . . . .	54
3.1	The SPIF #2 mock-up: (a) global view of the BF configuration; (b)-(c) bracing system and T-stub connections of the intervention; (d)-(e) front view of the 1 <sup>st</sup> and 2 <sup>nd</sup> floor at the EUCENTRE Laboratory. . . . .	68
3.2	(a) Acceleration spectra according to: EN 1998–1, black line; TH #8, gray line, used in the SPIF MRF testing campaign; GM7121, red line, adopted in the SPIF #2 BF testing campaign. (b)-(c) Relevant acceleration time histories of TH #8 and GM7121, respectively. . . . .	71
3.3	(a) Installed fin plate connections FP #1; (b) warping and crack propagation in the web of the crossbeam under Tank #2; and (c) strengthening intervention. . . . .	72
3.4	(a) Lateral view of the mock-up; (b) and (c) steel member layout, non structural components and instrumentation. . . . .	74
3.5	The SPIF #2 global FE model with relevant FE models of secondary components. . . . .	80

3.6	Selected records: (a) displacement; (b) velocity; and (c) acceleration response spectra. Grey lines refer to single records whereas black dashed lines indicate the corresponding 95% confidence interval. . . . .	84
3.7	a) Relevant frequency variations for the BF mock-up. Damping ratio box-plots are reported with whiskers referring to the 10 <sup>th</sup> and 90 <sup>th</sup> -quantile; b) mode shapes relevant to frequencies $f_n = 4.50, 6.83, 7.84$ and $10.04\text{ Hz}$ of Table 3.5. . . . .	91
3.8	a) Photo of a buckled brace; b) axial forces time history at GM7121#62% and (c) at GM7121#115%. . . . .	92
3.10	Pos.#1 BFJ: (a) sketch of the cross section; (b) photo of the monitored BFJ on site. . . . .	96
3.11	Leakage predictions and interaction domains with and w.o. safety factors for (a) DBE and (b) SSE condition. . . . .	97
3.12	Seismic input vs primary structure correlation data: (a) $PGA$ vs $Sa_{floor}(T_1)$ as spectral QoI; (b) $PGA$ vs $\max D_{top} $ as non-spectral QoI. Collections of * and $\triangle$ data represent results for MRF and BF configuration, respectively. Shaded dots indicate processed data after inelastic behaviour occurred. . . . .	99
3.13	Seismic input vs NSCs correlation data: $E - ASA_R(f_1)$ vs (a) $Sa_{floor}(T_{NSC})$ ; (b) $E - ASA_R(f_1)$ vs $\max D_{R,Tank\#1} $ . Collections of * and $\triangle$ data represent results for MRF and BF configuration, respectively. Shaded dots indicate processed data after inelastic behaviour occurred. . . . .	100
3.14	Primary structure vs NSCs correlation data: (a) $Sa_{floor}(T_1)$ vs $S_{V,Tank\#1}$ ; (b) $Sa_{floor}(T_1)$ vs $\max D_{R,Tank\#1} $ . Collections of * and $\triangle$ data represent results for MRF and BF configuration, respectively. Shaded dots indicate processed data after inelastic behaviour occurred. . . . .	100
4.1	(a) FBJ Sensor placement for the sliding/uplifting monitoring of unanchored storage tanks; (b) example of inlet/outlet pipes of a storage tank. . . . .	114
4.2	(a) FBJ sensor layout for columns; (b) FBJ sensor layout for vertical elevated vessels; (c) FBJ layout for horizontal pressure vessels. . . . .	116
4.3	Case study #1: tank-piping system and secondary components, (after Sayginer 2020 [18]) . . . . .	118
4.4	Main dimensions of specimen and flange joint. . . . .	119

---

4.5	(a) Sensor layout for the flange monitoring (b) Sensors installed on the specimen. . . . .	121
4.6	(a) Joule-Thomson effect during the validation test, (b) test setup of the validation test. . . . .	122
4.7	(a) Experimental setup (b) Liquid pressure system. . . . .	123
4.8	Top displacements history. . . . .	125
4.9	Force-displacement relationship. . . . .	125
4.10	(a) Deformation evolution measured by strain-gauges; (b) relative displacement histories of the flange joint measured by LVDTs. . . . .	126
4.11	Moment – Rotation relationship of the BFJ. . . . .	128
4.12	Leakage domain of the BFJ (after Bursi et al., [41]). . . . .	128
4.13	(a) Deformation measured by FBGs (b) Relative displacements of the flange joint measured by FBGs. . . . .	129
4.14	Case study #2: Mock-up photographs at the EUCENTRE Laboratory (after Butenweg et al 2020, [43]). . . . .	130
4.15	(a) Piping layout and (b) flange joints details. . . . .	131
4.16	(a) Traditional sensors Layout (b) GS4LD optic fibers based Leakage Detection transducer installed on one of the two pressurized vessels mounted on the EUCLID shaking platform in Pavia. . . . .	133
4.17	(a) Time history relations of flange opening recorded by LVDTs; (b) time history relations for flange opening recorded by FBG sensors. . . . .	134
5.1	Photos of the SPIF's mock-up @EUCENTRE, Pavia: a) the MRF configuration; b) the two installed vertical tanks; c) details of the BFJ between vertical tank and piping system at 1 <sup>st</sup> level; d) the BF configuration. . . . .	147
5.2	FE global models in SAP2000 <sup>®</sup> : a) the global MRF model; b) the global BF model; c) local HF models and their locations in a) and b). . . . .	148
5.3	Fin plate: a) CBFEM strain analysis results; b) photos of the crack initiation on the mock-up. . . . .	149
5.4	Base joint: a) semi-rigid joint classification, according to §5.2.2.5(2) of EN 1993-1-8 [26]; b) CBFEM of IDEA StatiCa <sup>®</sup> stress analysis results. . . . .	150
5.5	FE model discretization: (a) mesh size and element selected list; (b) mesh visualization and labels. . . . .	151
5.6	FE model results <i>via</i> ANSYS <sup>®</sup> of BFJ: a) deformation analysis; b) plastic strain analysis. . . . .	152

5.7	Leakage predictions and interaction domains with and w.o. safety factors for SSE in (a) MRF and (b) BF configurations. . . . .	154
5.8	Local high fidelity models for (a) vertical and (c) horizontal tanks; (c) simplified stick models of the vertical and horizontal tanks. . . . .	155
5.9	Numerical and experimental a) acceleration TH 1st floor MRF b)acceleration TH tank#1 floor MRF . . . . .	160
5.10	Numerical and experimental a) acceleration TH 1st floor BF b)acceleration TH tank#1 floor BF . . . . .	161
5.11	Dialog box of the Matlab applications: a) MatHazard for PSHA, b) SCoRes for record selection . . . . .	163
5.12	a) Target UHS for different return periods $T_R$ , b) Seismic hazard curves of Amatrice(Italy) . . . . .	164
5.13	Spectra of the 30 unscaled accelerograms selected for the hazard level $T_R = 475$ years, spectra of their logarithmic mean and the mean + 1 std compared with the target spectra. . . . .	167
5.14	Maxima bottom-wall strain and acceleration experimental measures collected for Tank #1 and linear interpolation model with confidence bounds of 95%; $\max (\varepsilon)  = \varepsilon_y$ threshold separating DBE from SSE limit state, according to [6]. . . . .	168
5.15	(a) fragility curves for DBE for MRF and BF set A and set B (b) fragility curves for SSE for MRF and BF set A and set B . . . . .	170
5.16	(a) fragility curves for DBE for MRF and BF set A and set B (b) fragility curves for SSE for MRF and BF set A and set B for Tank#2 . . . . .	171
6.1	Steps of the global theoretical framework for UQ. . . . .	183
6.2	Heuristics $\mathcal{A}_{1-2}$ : substeps for computational model, (i) FEM physics-informed and (ii) PCE meta-model. . . . .	184
6.3	Heuristics $\mathcal{B} - \mathcal{C}$ : substeps for input parameter description and post-processing of responses UQ forward analyses. . . . .	184
6.4	Scree plot for the GMM generated gms meta-features. . . . .	188
6.5	(a) Schematics of the simplified 3DoF system; (b) Bouc-Wen hysteresis for 1 <sup>st</sup> DoF of the simplified system. . . . .	193

---

6.7	The SPIF #2 mock-up: (a) photo of the braced frame configuration on the shake table of EUCENTRE Facilities and detail of the vertical tank installed at the first level; (b) SAP2000®FE model and focus on the vertical tank <i>ad-hoc</i> implemented stick-model. . . . .	195
6.8	Monte Carlo derived state-dependent fragility functions: grey lines represent single simulations; dashed-dark red lines depict the 50% and 90% confidence bounds, whilst continued-dark red ones the 99%. Lighter to darker shaded areas highlighted the corresponding regions of the aforementioned quantiles. . . . .	198
6.9	Comparison of the output given by the reference model ( $Y_{ED_0} = \mathcal{M}(\mathbf{X})$ ) and the PCE model ( $\hat{Y}_{PCE_0} = \mathcal{M}^{PC}(\mathbf{X})$ ).200	
6.10	Comparison of the output given by the reference model ( $Y_{ED_1} = \mathcal{M}(\mathbf{X})$ ) and the PCE model ( $\hat{Y}_{PCE_1} = \mathcal{M}^{PC}(\mathbf{X})$ ).200	
6.11	Bootstrapped-PCE derived state-dependent fragility functions: grey lines represent single simulations; dashed-dark red lines depict the 50% and 90% confidence bounds, whilst continued-dark red ones the 99%. Lighter to darker shaded areas highlighted the corresponding regions of the aforementioned quantiles. . . . .	202
6.12	(a) Histogram distribution of the surrogate initial condition '0' outputs (red) <i>vs</i> original data of the ED; (b) control plot of the performance of the surrogate-'0'model <i>vs</i> the true ED samples. . . . .	204
6.13	(a) Histogram distribution of the surrogate damage condition '1' outputs (red) <i>vs</i> original data of the ED; (b) control plot of the performance of the surrogate-'1'model <i>vs</i> the true ED samples. . . . .	204
6.14	Bootstrapped-PCE state-dependent fragility curves of the SPIF #2 vertical tank: dark-red thick lines stand for the 50%, 90% and 99% confidence bound, along with lighter to darker shaded areas. . . . .	205
6.15	Transition state '1-2': on the left, the histogram of the ED dataset and the inferred Gumbel PDF; on the right, log-normal, Gumbel and empirical CDFs. . . . .	207
6.16	Log-normal, inferred and empirical CDFs of the entire set of transition states fragility functions for the NSC of SPIF#2, with E – ASA <sub>R<sub>67</sub></sub> as IM. . . . .	208
6.A1	Histograms and distributional models for IMs: 1 to 10. .	211
6.A2	Histograms and distributional models for IMs: 11 to 20. .	212
6.A3	Histograms and distributional models for IMs: 21 to 30. .	213

6.A4	Histograms and distributional models for IMs: 31 to 40.. .	214
6.A5	Histograms and distributional models for IM 41. . . . .	215
6.A6	Correlation map between input IM parameters. . . . .	215
6.B1	Transition state '0-0': on the left, the histogram of the ED dataset and the inferred Gamma PDF; on the right, log-normal, Gumbel and empirical CDFs. . . . .	216
6.B2	Transition state '0-1': on the left, the histogram of the ED dataset and the inferred Weibull PDF; on the right, log-normal, Gumbel and empirical CDFs. . . . .	216
6.B3	Transition state '0-2': on the left, the histogram of the ED dataset and the inferred Gamma PDF; on the right, log-normal, Gumbel and empirical CDFs. . . . .	217
6.B4	Transition state '1-1': on the left, the histogram of the ED dataset and the inferred Gumbel PDF; on the right, log-normal, Gumbel and empirical CDFs. . . . .	217
6.B5	Transition state '1-2': on the left, the histogram of the ED dataset and the inferred Gumbel PDF; on the right, log-normal, Gumbel and empirical CDFs. . . . .	217
A1	Markov chain for structural damage transitions: from 0, undamaged, to C, collapsed. . . . .	230
A2	Damage accumulation due to sequence of seismic events, as a Markovian process, described in [3]. . . . .	231



## List of Tables

2.1	Sensors type and numbers in the mock-up . . . . .	27
2.2	Significant limit states for primary structures. . . . .	30
2.3	Significant limit states for process plants. . . . .	30
2.4	Nomenclature, characteristics and synthetic observations of SPIF Test Programme. . . . .	33
2.5	Identified frequencies from Random signals through PSDs analyses along the MRF direction. Also $\Delta[\%]$ variations between current and initial frequencies are reported. . . . .	35
2.6	Identified frequencies from Random signals through PSDs analyses along the BF direction. Also $\Delta[\%]$ variations between current and initial frequencies are reported. . . . .	35
2.7	Identified frequencies by the RFP's signal analysis on the TH #8 excitation both for the MRF and BF directions. The horizontal line separates OBE from SSE seismic in- puts. . . . .	38
2.8	Piping system w.r.t. Fig. 2.10 and response . . . . .	41
2.9	Comparison of floor response spectra ordinates at the fundamental period of Tanks #1 and #3 . . . . .	56
3.1	Limit states and performance objectives for industrial plants. . . . .	77
3.2	Recorded natural seismic events for the GMM's dataset.	83
3.3	Values of probabilities density distributions of GMM's parameters. . . . .	86
3.4	Nomenclature. Characteristics and synthetic observa- tions of the SPIF #2 Test Programme. . . . .	87
3.5	Identified frequencies by means of the RFP's signal anal- ysis on the GMM7121 excitation for both the BF seismic and orthogonal direction. The horizontal line separates DBE from SSE seismic inputs. Also $\Delta[\%]$ variations be- tween current and initial frequencies are reported. . . . .	89
3.6	Mass values and $\mu$ ratios. . . . .	95
3.7	Modal masses and $\mu_{mod}$ ratios. . . . .	95
3.8	Experimental EDP values and observed damage. . . . .	101
5.1	Probabilities density distributions of the updating param- eters for the MRF configuration: prior and posterior pa- rameters and type of distribution for each $\theta_i$ . . . . .	158

---

5.2	Probabilities density distributions of the updating parameters for the BF configuration: prior and posterior parameters and type of distribution for each $\theta_i$ . . . . .	158
5.3	Relevant model frequencies: numerical, i.e. evaluated through FE models; experimental, i.e. identified with rational fraction polynomials based on frequency response; $\Delta$ percentage as $(f_{n,exp} - f_{n,num}) / f_{n,exp} \cdot 100$ for (a) the MRF and (b) the BF configurations. . . . .	159
5.4	NEE values for the peak accelerations of Tank#1-#2 for (a) MRF configuration and (b) BF configuration. . . . .	162
5.5	List of records selected for the hazard level $T_R = 475$ years. Set A . . . . .	166
5.6	Reference limit states . . . . .	168
5.7	Mean annual frequency of exceedance for (a) at DBE and (b) SSE limit state conditions for Tank #1. . . . .	172
5.8	Mean annual frequency of exceedance for (a) at DBE and (b) SSE limit state conditions for Tank #2. . . . .	172
6.1	Probabilities density distributions of GMM's parameters. . . . .	186
6.2	A comprehensive list of ground motion IM parameters [18]- [31]. . . . .	187
6.3	Bouc-Wen parameters for the simplified 3DoF system. . . . .	193
6.4	Transition states for SPIF #2: classification based on the initial-final reached damage level limit state. Size population of each cluster and its fragility definition. . . . .	194
6.5	Transition states for the Bouc-Wen MDOF: classification based on the initial-final reached damage level limit state. Size population of each cluster and its fragility definition. . . . .	196
6.6	Monte Carlo state-dependent fragility functions: the top four $\beta_{eff}$ efficiency indices for each transition states. . . . .	199
6.7	Bootstrapped-PCE state-dependent fragility functions: the top four $\beta_{eff}$ efficiency indices for each transition states. . . . .	201
6.8	$\Delta(\beta_{eff})$ efficiency indices for each transition states. . . . .	203
6.9	Bootstrapped-PCE state-dependent fragility functions for the SPIF #2 NSC: the top five $\beta_{eff}$ efficiency indices of IMs for each transition states. . . . .	206
6.10	Summary of the log-normal distribution parameters and of the inferred distributions and their fitted parameters for each fragility function of the SPIF#2 NSC. . . . .	207
6.A.1	Histograms and distributional models for IMs. . . . .	210

## List of abbreviations and notations

### ▪ Chapter 1:

ATC	Applied Technology Council
DS	Damage State
FEM	Finite Element Model
IM	Intensity Measure
LRFD	Load and Resistance Factor Design
MH	Metropolis Hastings
NIST	National Institute of Standards and Technology
NSC	Non Structural component
PBEE	Performance Based Earthquake Engineering
PCE	Polynomial Chaos Expansions
PSHA	Probabilistic Seismic Hazard Analysis
QoI	Quantity of Interest
UQ	Uncertainty Quantification

### ▪ Chapter 2:

ASD	Allowable Stress Design
BF	Braced Frame
BFJ	Bolted Flange Joint
DBE	Design Basis Earthquake
FE	Finite Element
FFT	Fast Fourier Transform
FIR	Finite Impulse Response
FRF	Frequency Response Function
FRS	Floor Response Spectra
LoC	Loss of Containment
LRFD	Load and Resistance Factor Design
MRF	Moment Resisting Frame
NC	Near Collapse
OBE	Operating Basis Earthquake
PBD	Performance Based Design
PBEE	Performance Based Earthquake Engineering
PGA	Peak Ground Acceleration
PSD	Power Spectral Density
QRA	Quantitative Risk Analysis
RC	Reinforced Concrete

---

RFP	Rational Fraction Polynomial
RMS	Root Mean Square
RND	Random
SERA	Seismology and Earthquake Research Alliance
SG	Strain Gauge
SI	System Identification
SIMO	Single Input Multiple Output
SPIF	Seismic Performance Industrial Facilities
SSE	Safe Shutdown Earthquake
UNITN	University of Trento

▪ **Chapter 3:**

ASD	Allowable Stress Design
BF	Braced Frame
BFJ	Bolted Flange Joint
DBE	Design Basis Earthquake
DP	Deaggregation Probabilistic
FRF	Frequency Response Function
FRS	Floor Response Spectra
FO	Fully Operational
GMM	Ground Motion Model
HR	Hazards Reduced
INGV	Istituto Nazionale di Geofisica e Vulcanologia
ITACA	Italian Accelerometric Archive Database
LRFD	Load-and-Resistance Factor Design
LF	Low Fidelity
LS	Life Safety
MRF	Moment Resisting Frame
NC	Near Collapse
NIST	National Institute of Standards and Technology
NSC	Non-Structural Component
PBEE	Performance-Based Earthquake Engineering
PGA	Peak Ground Acceleration
PR	Position Retention
QoI	Quantities of Interests
SG	Strain Gauges
SHA	Seismic Hazard Analysis
SI	System Identification

RFP	Rational Fraction Polynomial
RND	Random
SSE	Safe Shutdown Earthquake
TMD	Tuned Mass Damper

▪ **Chapter 4:**

AET	Acoustic Emission Technique
API	American Petroleum Institute
BFJ	Bolted Flange Joint
FBG	Fiber Bragg Grating
FIR	Finite Impulse Response
ISO	International Organization for Standardization
LD	Leakage Detection
LoC	Loss of Containment
MEMS	Micro-Electro-Mechanical-System
NDT	Non-Destructive Techniques
OF	Optical Fiber
RFID	Radio Frequency Identification
SG	Strain Gauges
SLED	Super Luminescent LED

▪ **Chapter 5:**

BF	Braced Frame
BFJ	Bolted Flange Joint
CBF	Concentrically Braced Frame
CBFEM	Component-Based Finite Element Model
CDF	Cumulative Distribution Function
DBE	Design Basis Earthquake
EDP	Engineering Demand Parameter
FEMU	Finite Element Model Updating
LoC	Loss of Containment
GMPE	Ground Motion Prediction Equation
IM	Intensity Measure
MAC	Modal Assurance Criterion
MAF	Mean Annual Frequency

---

MC	Monte Carlo
MCMC	Monte Carlo Markov Chain
MH	Metropolis-Hastings
MRF	Moment Resistant Frame
NSC	Non-Structural Component
PBED	Performance-Based Earthquake Design
PGA	Peak Ground Acceleration
PSHA	Probabilistic Seismic Hazard Analysis
QRA	Quantitative Risk Analysis
RFP	Rational Fraction Polynomial
SPIF	Seismic Performance of Industrial Facilities
SSE	Safe Shutdown Earthquake
TH	Time-History
TMD	Tuned Mass Damper
UHS	Uniform Hazard Spectrum

▪ **Chapter 6:**

AIC	Akaike Information Criterion
AS	After Shock
BF	Braced Frame
CP	Collapse Prevention
DBE	Design Basis Earthquake
DoF	Degree of Freedom
DS	Damage State
ED	Experimental Design
EDP	Engineering Demand Parameter
IM	Intensity Measure
IO	Immediate Occupancy
IRF	Impulse Response Function
MLE	Maximum Likelihood
MS	Main Shock
NLTHA	Non Linear Time History Analyses
NSC	Non Structural Component
PBEE	Performance Based Earthquake Engineering
PCA	Principal Component Analysis
PC	Principal Component
PCE	Polynomial Chaos Expansions
PSHA	Probabilistic Seismic Hazard Analysis

SNLTHA	Sequential Non Linear Time Histories Analyses
SPIF	Seismic Performance of Industrial Facilities
SS	Seismic Sequence
SSE	Safe Shutdown Earthquake
UQ	Uncertainty Quantification



## 1. Introduction

### 1.1 Background and motivation

Earthquakes are among the most destructive natural disasters. Increasing urbanisation and the accumulation of civil and industrial assets in severe seismic-prone zones have led to greater exposure to earthquake hazards worldwide, [1]. Over the past decade, a series of strong earthquakes - *e.g.* Tohoku 2011, Emilia 2012, New Zealand 2016 - have caused loss of life and inflicted catastrophic damage in several regions, leading to unprecedented reconstruction and retrofitting intervention costs. Losses include both damages to buildings and business interruptions. However, the indirect costs and consequences of the latter can be far-reaching, [2]. The losses inflicted on businesses by earthquakes, indeed, can devastate the industry and the economy in general. Damaged buildings, machinery and equipment are generally costly to repair, and the scale of resulting business interruption losses can be very high and relatively difficult to estimate.

Focusing on the industry world, from the last decade of major earthquake disasters, a key realisation has been that non-structural components (NSCs) of industrial plant facilities have been a significant driver for overall physical damage and disruption to business. To this scope, the Applied Technology Council (ATC) under the National Institute of Standards and Technology (NIST) invested in a year-long study to collect and document the body of available knowledge related to the seismic performance of NSCs, summarized in [3]. From these studies, it clearly emerges: (i) a large adoption of classical load-and-resistance factor design (LRFD) and code-compliant methods often dated and inadequate, as highlighted also in [4]-[5]; (ii) a gap in performing fully comprehensive testing campaigns and investigations on coupling effects between primary structures and NSCs; (iii) a need to improve and enforce code requirements along with the development of reliable NSCs seismic demands models. More precisely, codes and regulations establish the minimum requirements for structures to resist the effects of earthquakes with defined probability levels (or return periods), providing a basic level of seismic risk reduction. The primary objective of codes and regulations on structures is to save lives, not the structures themselves. When properly implemented, codes have significantly reduced the loss of life in major seismic events in recent years. However, from the perspective of economic resilience, the enormous scale of associated financial losses requires a paradigm shift. Encouragingly, in recent times,

---

earthquake building codes have been revised to implement elements of a performance-based earthquake engineering (PBEE) framework to address issues of damage limitation and reparability as well as life safety.

Based on the definition of PBEE stated in the Structural Engineers Association of California (SEAOC) Vision 2000 document [6], the first step in PBEE is to determine and select the performance objectives (PO), i.e. the link between expected performance levels and seismic ground motion intensities. In more detail, a performance level represents a distinct band in assessing damage to the overall structural and NSCs elements that also considers the consequences of the damage to the occupants and functions of the facility, [7]. POs typically include multiple goals for the performance of the constructed facilities. To this scope, Figure 1.1 initially presented in the SEAOC document [6], illustrates the PBEE framework applied to engineering facilities. A discrete set of pre-defined system POs and a set (discrete or continuous) of seismic hazard levels are represented on the two axes of the schematics. The domain defined by the two axes is then partitioned into two subdomains, the acceptable domain and its complement, the not acceptable. Within the acceptable domain, designers and stakeholders define the desired combination of POs w.r.t. the hazard level and its likelihood and the monetary cost of the system. According to this scheme, four discrete performance levels are identified and linked to earthquake design levels. Thus, the selection of POs sets the acceptability criteria for the design, i.e. the rules and guidelines to satisfy in order to ensure the operativity, safety, and business performance objectives.

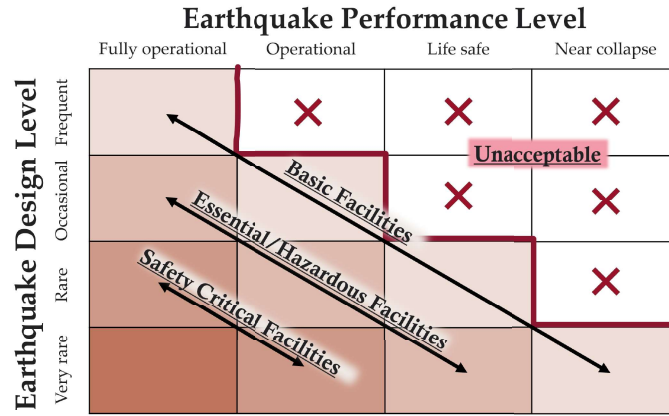


Figure 1.1: PBEE schematics: minimum seismic performance objectives coupled with earthquake levels for buildings, according to [7].

Also, SEAOC Vision 2000 describes various hazard levels with spe-

cific return periods: (1) the frequent intensity level with a 50% exceedance probability in 30 years, (2) the occasional intensity level with a 50% exceedance probability in 50 years, (3) the rare intensity level with a 10% in 50 years, and (4) the very rare intensity level with a 10% in 100 years.

Similarly, FEMA 365 “Prestandard and Commentary for the Seismic Rehabilitation of Buildings” [8] provides professional engineers with a tool for designing seismic rehabilitation measures for existing structures in a PBEE perspective. Indeed, the document defines various target building performance levels and earthquake hazard levels similar to those presented in SEAOC Vision 2000 by means of quantitative tables and qualitative descriptions of corresponding physical damage for both structures and NSCs.

Along the same line, in 1997 the Pacific Earthquake Engineering Research Center (PEER) decided to develop a more robust methodology for PBEE. The PEER PBEE framework developed by PEER facilitates direct calculation of the effects of uncertainty and randomness on each step in the performance-based procedure.

The framework is simply a statement of the total probability theorem for a selected decision variable’s yearly mean number of events. In specific, the so-named PEER formula was originally written as follows:

$$\lambda(dv) = \int_d \int_{im} G(dv|d)|dG(d|im)||d\lambda(im)| \quad (1.1)$$

and later rewritten as

$$\lambda(dv) = \int_d \int_{edp} \int_{im} G(dv|d)|dG(d|edp)||dG(edp|im)||d\lambda(im)| \quad (1.2)$$

where *IM* (intensity measure), *EDP* (engineering demand parameter), *D* (damage state), and *DV* (decision variable) are continue random variables describing respectively the hazard intensity, the structural response, the state of the structure, and a suitable decision variable for decision making.  $\lambda(x)$  is the mean annual rate of events exceeding a given threshold for a given variable  $x$ , and  $G(y|x) = P(Y \geq y|X = x)$  is the conditional complementary cumulative distribution function (CCDF). Figure 1.2 shows the four steps into which the seismic assessment is deconstructed.

In this respect, the PBEE PEER framework has gained momentum above all to perform seismic risk analyses, thanks to its inherent versatility, [9]. Its strength, indeed, relies on the simple yet effective implementation of the total probability theorem, which allows to decouple and then combine the output of probabilistic seismic hazard analysis (PSHA) with fragility, damage, and loss analysis.

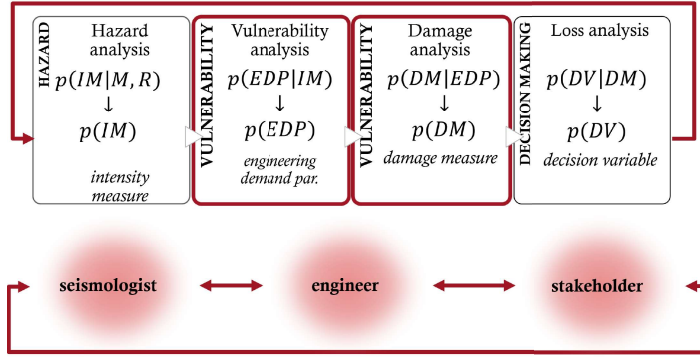


Figure 1.2: The PEER-PBEE schematics.

The huge structural damages caused by strong earthquakes, such as in the 1989 Loma Prieta, the 1994 Northridge, the 1999 Chi-Chi, Taiwan, the 1999 Kocaeli and 2011 Tohoku, Japan, earthquake [10]-[11]-[12], demonstrate that a dependable evaluation of seismic hazard appears of paramount importance. The definition of the levels of earthquake motions to be considered for analysis requires special attention. Several standards dealing with the seismic analysis of process plant components, e.g., NFPA 59A [13], in view of enhanced performance and damage limitation, use the same seismic hazard definitions adopted by nuclear standards NEA/CSNI/R (2007)17 [14]. These standards prescribe two different limit states: the design basis earthquake (DBE) and the safe shutdown earthquake (SSE). Nevertheless, intended safety objectives are different: in fact, (i) conventional facilities are designed for human lives protection and damage limitation [15]; conversely, (ii) NPPs rules enforce integrity and functionality of structures systems and safety-critical components; as a result, inelastic behaviour is not allowed. Thus, in moderate seismicity regions, a correspondence between the 10% probability of exceedance in 50 years, i.e., 475 years return period used in Eurocode 8 [15], and the design basis earthquake ground motion defined in nuclear standards can be established. Increased return periods can be achieved through the importance factors. Safe shutdown earthquake ground motion is usually defined according to rules properly defined for the special-risk industries. Therefore, the definition of the corresponding return periods for the design/assessment of process plants is more involved [16]. In any case, a full probabilistic seismic hazard analysis (PSHA) of the site is necessary. The hazard analysis provides the probability of exceeding a selected intensity measure (IM) value in a given

time interval. For the construction of fragility curves, it is often necessary to use nonlinear analysis, which requires seismic motion records [17]. If a scalar IM is used, such as the peak ground acceleration or spectra acceleration at the fundamental period ( $Sa(T)$ ), the correlation with the response, expressed in terms of engineering demand parameters (EDPs), is generally low as shown in [18]. Thus, further uncertainty is introduced in addition to the attenuation law's uncertainty. Similar remarks can be made if the ground motion records are selected on the basis of a given range of frequencies usually provided by a target uniform hazard spectrum (UHS); see, in this respect, [19]. As an alternative, accelerograms whose spectrum individually matches the UHS could be used. These records can be artificially built or obtained by modifying, with appropriate techniques, the frequency content of records. The first approach has been completely abandoned, while the second one still represents an interesting alternative [20]-[21]. However, process plant components are often characterized by a variegated frequency content. This clearly complicates the problem of the accelerogram selection. In civil engineering, where complex constructions exhibit similar problems, vector-valued IMs have been defined [22].

To assess seismic risk, the aforementioned fragility analysis step offers the critical link between seismic hazard and structural modelling, since it estimates the conditional probability of exceeding or attaining a certain damage state (DS) given an intensity measure (IM) of earthquake motion. In this regard, a growing number of studies, the increase of community-funded research projects and experimental campaigns focused on unfolding the complex and highly diverse behaviour of these process components. For example, the European research project INDUSE-2-SAFETY 2012-2015 [23], investigated through experimental tests the performances of several NSCs and their limit state levels to be compliant with. Conversely, the United States Nuclear Regulatory Commission agency carried out a multi-year test programme to better understand the elastoplastic response and ultimate strength of nuclear power piping systems, [24]. As a result, in view of the enhancement of structural integrity of industrial, energy and nuclear components as well as fitness for service, design guidelines and recommendations were issued [25] - [26].

However, the problem's complexity and its inherent modelling, coupled with a general scarcity of available data and the model's limited capability, concurred in limiting or developing risk assessment methods based on meaningful reduced and quick-to-run models. Indeed, the computation of fragility curves requires a realistic estimation of the structure performance subjected to seismic excitations *via* the quantification and

---

propagation of uncertainties existing in seismic ground motions, structural material properties and so on. Thus, it requires hundreds of heavy numerical FE model simulations. Recently, new studies regarding the application of metamodels or surrogate models in fragility analysis have been realized. Most of them focus on using seismic intensity measures (IMs) to characterize earthquakes. Metamodels are then constructed to calibrate the relation between damage measures (DMs) and uncertain inputs of the structural models, including IMs and structural parameters. Among surrogate families that provide more than just an approximation to the model, polynomial chaos expansions (PCE) [27], Kriging, or Gaussian process modelling [28]-[29], support vector machines, artificial neural networks [30]-[31]-[32] became the most popular in the civil engineering domain. For example, they might additionally yield analytical estimates of the moment response model, sensitivity indices or confidence levels for their predictions.

Moreover, in recent years, also several novel methodological contributions to fragility analysis have been made that include: i) the development of multivariate fragility functions [31]; ii) the introduction of seismic fragility analysis based on a combination of artificial ground motions and surrogate modeling [28]-[33]; iii) the consideration of both state and time-dependent fragility [34]-[35]. On the latter point, Iervolino et al. [36] focused on the estimation of state-dependent fragility curves, which are fragility models that allow for the possibility that a structure may have already been damaged by previous shocks. To overcome the computational cost of the methodology, the authors proposed a solution applicable to reinforced concrete single degree of freedom (SDOF) systems, calibrated through pushover analyses [37] and based on discrete-time homogenous Markovian process. In particular, the fragility functions, or probabilities of transition from a damage limit state to a severe one, are interpreted as the element of a Markovian transition matrix, [38]-[36].

## 1.2 Objectives of the thesis and core contribution

On these premises, this dissertation aims to develop an innovative, efficient and accurate framework for evaluating state-dependent fragility functions for critical industrial process components. The relevant vulnerability assessment is based on the integration of data derived from an intensive experimental campaign, accomplished within the European SERA SPIF project, with the computational potential obtained from the most advanced metamodeling techniques available. The intrinsic value of this framework resides in the experimental data on which it is built

and implemented. These are the offspring of the comprehensive experimental programme completed at the EUCENTRE laboratories in Pavia. In particular, the tests carried out on a shaking table of two archetypes of industrial systems full-scale steel substructures, equipped with NSCs such as tanks, cabinets, BFJs, and piping elements, represents an added values of the thesis. In fact, experimental data fill the gap in terms of experimental evidence of tests conducted in a PBEE framework capable of taking into account the effects of NSCs-primary structure coupling as a whole.

Therefore, another added value of the thesis lies in the performance evaluation and study of the complex interactions between NSCs and the primary structures through the development of different highly refined numerical models capable of capturing interaction effects. They are conceived to be quicker and inexpensive-to-run and able to capture the global behaviour of each coupled system.

### **1.3 Organization of the thesis**

The thesis presents the experimental and numerical research the Author performed during her PhD programme, along with the relevant analytical findings and achievements. Thus, the thesis is organized as follows.

Chapter 1 provides a concise overview of the problem and the statement of the research objectives. It includes the experimental shake table test campaigns and the vulnerability seismic assessment for special risk industrial substructures.

The subsequent Chapters 2 and 3 move into the core of the experimental research activity. Drawing on papers already published by the Author and her research group, the comprehensive shake table test campaigns of the two most widespread steel frame configurations for industrial plant substructures are presented. In detail, Chapter 2 presents the shake table tests of a moment resisting frame structure excited by an EC8-spectrum-compatible accelerogram. Then, Chapter 3 describes the experimental campaign carried out by means of a synthetic seismic input, derived from a site-based ground motion model, on the same mock-up converted into a braced frame configuration, thanks to *ad-hoc* design and installation of a seismic retrofitted bracing system.

Within the experimental domain, Chapter 4 provides insights into the performance of an innovative fiber-optic monitoring system, which was deployed and tested during the shake table tests, for one of the most critical components in major-hazard industrial facilities: a bolted-flange joint.

---

Chapter 5 discusses the analytical and numerical models developed: (*i*) to monitor the experimental campaign; (*ii*) to better interpret the physical phenomena that governed the dynamic behaviour of the coupled system; and (*iii*) to perform seismic risk analyses of non-structural components. For this purpose, particular emphasis is devoted to developing a simple global model that is calibrated on complex local high-fidelity models and balances the accuracy of results with the computational-time burden.

Along this vein, Chapter 6 discusses an innovative framework for the formulation of state-dependent fragility curves that combines experimental data with the most advanced computational metamodeling tools, in a forward uncertainty quantification (UQ) perspective. By leveraging the latter, expensive-to-evaluate computational models, e.g., FE models, are substituted with inexpensive-to-evaluate surrogates, preserving the required accuracy for the quantity of interest (QoI) investigated.

The findings are finally summarized in Chapter 7, where the main research results are underlined together with future perspectives.

## Bibliography

- [1] SwissRe-Institute, “*A decade of major earthquakes: lessons for business,*” 2019.
- [2] E. Krausmann, E. Renni, M. Campedel, and V. Cozzani, “Industrial accidents triggered by earthquakes, floods and lightning: Lessons learned from a database analysis,” *Natural Hazards*, vol. 59, 2011.
- [3] NIST GCR 18-917-43, “Recommendations for Improved Seismic Performance of Non-Structural Components,” 2018.
- [4] M. De Biasio, S. Grange, F. Dufour, F. Allain, and I. Petre-Lazar, “Intensity measures for probabilistic assessment of non-structural components acceleration demand,” *Earthquake Engineering & Structural Dynamics*, 2015.
- [5] P. Calvi, T. J. Sullivan, and R. Nascimbene, “Towards improved floor spectra estimates for seismic design.,” *Earthquake and Structures*, vol. 4, pp. 109–132, 2013.
- [6] S. V. . Committee *et al.*, “Performance-based seismic engineering,” *Structural Engineers Association of California, Sacramento, California*, 1995.

- [7] R. D. Bertero and V. V. Bertero, “Performance-based seismic engineering: the need for a reliable conceptual comprehensive approach,” *Earthquake Engineering & Structural Dynamics*, vol. 31, no. 3, pp. 627–652, 2002.
- [8] FEMA, “Prestandard and commentary for the seismic rehabilitation of buildings (fema356),” *Washington, DC: Federal Emergency Management Agency*, vol. 7, no. 2, 2000.
- [9] V. E. Saouma and M. A. Hariri-Ardebili, *Performance Based Earthquake Engineering*, pp. 517–528. Cham: Springer International Publishing, 2021.
- [10] A. M. Moat, J. T. A. Morrison, and S. Wong, “Performance of industrial facilities during 1999 earthquakes: Implications for risk managers,” *Global Change and Catastrophe Risk Management: Earthquake Risks in Europe, EuroConference, Laxenburg, Austria*, 2000.
- [11] M. Kazama and T. Noda, “Damage statistics (summary of the 2011 off the pacific coast of tohoku earthquake damage),” *Soils and Foundations*, 2012. Special Issue on Geotechnical Aspects of the 2011 off the Pacific Coast of Tohoku Earthquake.
- [12] R. Dobashi, “Fire and explosion disasters occurred due to the great east japan earthquake (march 11, 2011),” *Journal of Loss Prevention in the Process Industries*, 2014.
- [13] NFPA-59A, “Standards for the production, storage and handling of liquefied natural gas (LNG),” *Journal of Loss Prevention in the Process Industries*, 2013.
- [14] N. E. Agency, “Differences in approach between nuclear and conventional seismic standards with regard to hazard definition,” *CSNI Integrity and Ageing Working Group, Nuclear Energy Agency Committee on the Safety of Nuclear Installations, Organisation for Economic Cooperation and Development, Paris, France, Report No. NEA/CSNI/R(2007)17*, 2008.
- [15] E. 1998-1, “Eurocode 8: Design of structures for earthquake resistance—part 1: General rules, seismic actions and rules for buildings,” *British Standard EN, Brussels, Belgium*, 2005.
- [16] O. Bursi, F. Paolacci, and M. S. Reza, “Performance-based analysis of coupled support structures and piping systems subject to seismic loading,” 07 2015.

- 
- [17] E. I. Katsanos, A. G. Sextos, and G. D. Manolis, “Selection of earthquake ground motion records: A state-of-the-art review from a structural engineering perspective,” *Soil dynamics and earthquake engineering*, vol. 30, no. 4, pp. 157–169, 2010.
  - [18] H. N. Phan, F. Paolacci, and S. Alessandri, “Enhanced seismic fragility analysis of unanchored steel storage tanks accounting for uncertain modeling parameters,” *Journal of Pressure Vessel Technology*, vol. 141, no. 1, 2019.
  - [19] J. W. Baker and C. Allin Cornell, “A vector-valued ground motion intensity measure consisting of spectral acceleration and epsilon,” *Earthquake Engineering & Structural Dynamics*, vol. 34, no. 10, pp. 1193–1217, 2005.
  - [20] N. Abrahamson, “Non-stationary spectral matching,” *Seismological research letters*, vol. 63, no. 1, p. 30, 1992.
  - [21] S. Mukherjee and V. K. Gupta, “Wavelet-based generation of spectrum-compatible time-histories,” *Soil dynamics and Earthquake engineering*, vol. 22, no. 9-12, pp. 799–804, 2002.
  - [22] J. W. Baker, “Probabilistic structural response assessment using vector-valued intensity measures,” *Earthquake Engineering & Structural Dynamics*, vol. 36, no. 13, pp. 1861–1883, 2007.
  - [23] O. Bursi and R. di Filippo, “Component fragility evaluation, seismic safety assessment and design of petrochemical plants under design-basis and beyond-design-basis accident conditions,” tech. rep., Final Report, INDUSE-2-SAFETY Project, Contr. No: RFS-PR-13056, Research Fund for Coal and Steel, 2018.
  - [24] U.S.NRC, “Seismic Analysis of Large-Scale Piping Systems for the JNES-NUPEC Ultimate Strength Piping Test Program,” *Office of Nuclear Regulatory Research*, 2008.
  - [25] ASCE/SEI, *Seismic Analysis of Safety-Related Nuclear Structures*. Standard 4-16, 2016.
  - [26] U.S. Department of Energy, “Seismic Evaluation Procedure For Equipment in U.S. Department of Energy Facilities,” *Office of Defense Programs and Office of Environment, Safety and Health*, 1997.

- [27] C. V. Mai, *Polynomial chaos expansions for uncertain dynamical systems – Applications in earthquake engineering.* PhD thesis, ETH Zürich, Switzerland, 2016.
- [28] G. Abbiati, M. Broccardo, I. Abdallah, S. Marelli, and F. Paolacci, “Seismic fragility analysis based on artificial ground motions and surrogate modeling of validated structural simulators,” *Earthquake Engineering & Structural Dynamics*, 2021.
- [29] R. Gentile and C. Galasso, “Gaussian process regression for seismic fragility assessment of building portfolios,” *Structural Safety*, vol. 87, 07 2020.
- [30] A. Du, J. Cai, and S. Li, “Metamodel-based state-dependent fragility modelling for markovian sequential seismic damage assessment,” *Engineering Structures*, 2021.
- [31] A. Du and J. E. Padgett, “Investigation of multivariate seismic surrogate demand modeling for multi-response structural systems,” *Engineering Structures*, 2020.
- [32] Z. Wang, N. Pedroni, I. Zentner, and E. Zio, “Seismic fragility analysis with artificial neural networks: Application to nuclear power plant equipment,” *Engineering Structures*, 2018.
- [33] G. L. Yeo and C. A. Cornell, “A probabilistic framework for quantification of aftershock ground-motion hazard in california: Methodology and parametric study,” *Earthquake Engineering & Structural Dynamics*, vol. 38, no. 1, pp. 45–60, 2009.
- [34] J. Ghosh and J. E. Padgett, “Aging considerations in the development of time-dependent seismic fragility curves,” *Journal of Structural Engineering*, vol. 136, 2010.
- [35] R. Costa, T. Haukaas, and S. E. Chang, “Agent-based model for post-earthquake housing recovery,” *Earthquake Spectra*, vol. 37, no. 1, pp. 46–72, 2021.
- [36] I. Iervolino, M. Giorgio, and E. Chioccarelli, “Markovian modelling of seismic damage accumulation,” *Earthquake Engineering & Structural Dynamics*, 2015.
- [37] M. Orlacchio, G. Baltzopoulos, and I. Iervolino, “State-dependent seismic fragility via pushover analysis,” *17th World Conference on Earthquake Engineering, 17WCEE*, 2020.

- 
- [38] I. Iervolino and M. Giorgio, “Holistic modelling of loss and recovery for the resilience assessment to seismic sequences,” *Findings*, 2022.